Brief Communication

A Cytosolic Residue Mediates Mg^{2+} Block and Regulates Inward Current Amplitude of a Transient Receptor Potential Channel

Alexander G. Obukhov and Martha C. Nowycky
Department of Pharmacology and Physiology, New Jersey Medical School, University of Medicine and Dentistry of New Jersey, Newark, New Jersey 07103

Members of the transient receptor potential (TRP) cation channel family control a wide variety of cellular functions by regulating calcium influx. In neurons, TRP channels may also modulate cell excitability. TRPC5 is a neuronal TRP channel that plays a role in controlling neurite extension in the hippocampus. Transiently expressed TRPC5 exhibits a doubly rectifying current–voltage relationship characterized by relatively large inward currents and a unique outwardly rectifying current with a "flat" segment between +10 and +40 mV that may be attributable to Mg^{2+} block. We find that intracellular Mg^{2+} blocks the outward current through TRPC5 with an IC_{50} of 457 μM. The block is mediated by a cytosolic aspartate residue, D633, situated between the termination of the sixth transmembrane domain and the "TRP box." The substitution of noncharged or positively charged residues for the negatively charged D633 resulted in a channel with markedly reduced inward currents, in addition to decreased Mg^{2+} block. This suggests that electrostatic attraction of cations by D633 may contribute to inward current amplitude in TRPC5. We propose that cytosolic negatively charged residues can modulate the conductivity of TRP cation channels.

Key words: **TRP channels; cation channels; Mg^{2+} block; inward rectification; inward currents; calcium influx; cell excitability**

Introduction

Canonical transient receptor potential channels (TRPCs) are ubiquitous receptor-operated nonspecific cation channels that belong to the P-loop superfamily. By analogy with other channels, TRPCs are predicted to be tetramers formed from individual subunits with six transmembrane domains (Clapham, 2003). On activation, TRPCs may contribute to Ca^{2+} signaling and changes in cell excitability. TRPC5 channels are predominantly expressed in the brain (Riccio et al., 2002) and exist in homomeric form or as a heteromer combined with TRPC1 (Strübing et al., 2001; Greka et al., 2003; Bezzerides et al., 2004). TRPC5 may underlie metabotropic glutamate receptor-activated currents in the hippocampus and cerebellum, as well as regulate neurite extension in the hippocampus (Moran et al., 2004).

TRPC5 homomers and TRPC5/TRPC1 heteromers exhibit distinct complex current–voltage (*I–V*) relationships. TRPC5 has a doubly rectifying *I–V*, with relatively large inward currents. In contrast, TRPC5/TRPC1 is predominantly outwardly rectifying, with relatively small inward currents at negative potentials (Clapham, 2003). The *I–V* of TRPC5, but not TRPC5/TRPC1, exhibits an unusual segment between +10 and +40 mV, with near "zero" slope attributable to block by intracellular Mg^{2+} ($[Mg^{2+}]_i$) (Schaefer et al., 2000). At voltages more than +40 mV, the block is relieved.

In inwardly rectifying potassium channels (Kir), $[Mg^{2+}]_i$ block is attributable to interaction with negatively charged residues within the pore or in the cytosolic domain of the channel (Bichet et al., 2003). TRPC5 lacks anionic residues in the putative pore region. However, there are three negatively charged residues (D633, D636, and E638) situated near the predicted termination of the sixth transmembrane domain (TM6) (Dohke et al., 2004). To investigate the mechanism of Mg^{2+} block, we made single point mutations at these residues, expressed the channels, and performed voltage-clamp recording. We found that a single residue, D633, mediates Mg^{2+} block and contributes to the regulation of inward current amplitude.

Materials and Methods

Molecular biology/cell culture. The following clones were studied: TRPC5 (GenBank accession numbers AY064411 and AF060107), TRPC1 (GenBank accession number U73625), and H_1 histamine receptor (H_1R) (GenBank accession number D50095). The H_1 receptor fused to YFP (yellow fluorescent protein) served as a reporter cDNA. Mutations were generated using the QuickChange site-directed mutagenesis kit (Stratagene, La Jolla, CA). The nucleotide sequence of mutants was confirmed by sequencing. Human embryonic kidney 293 (HEK293) cells were cultured and transfected, as described previously (Obukhov and Nowycky, 2002, 2004).

Electrophysiology and analysis. Whole-cell currents were recorded in the episodic mode at −60 mV (sampled at 1 kHz; filtered at 3 kHz). Each episode lasted 5 s and contained a 200 ms ramp from −100 to +100 mV. The first *I–V* that followed the peak of the histamine-activated current at

Received July 22, 2004; revised Nov. 30, 2004; accepted Dec. 9, 2004.

This work was supported by an American Heart Association National Scientist Development grant (A.O.G.) and a National Institutes of Health and Muscular Dystrophy Association grant (M.C.N.). We thank the New Jersey Medical School Molecular Resource Facility for synthesis of primers and sequencing.

Correspondence should be addressed to Dr. Alexander G. Obukhov, Department of Pharmacology and Physiology, New Jersey Medical School, University of Medicine and Dentistry of New Jersey, 185 South Orange Avenue, Newark, NJ 07103. E-mail: oboukhal@umdnj.edu.

DOI:10.1523/JNEUROSCI.4451-04.2005

Copyright © 2005 Society for Neuroscience 0270-6474/05/251234-06$15.00/0

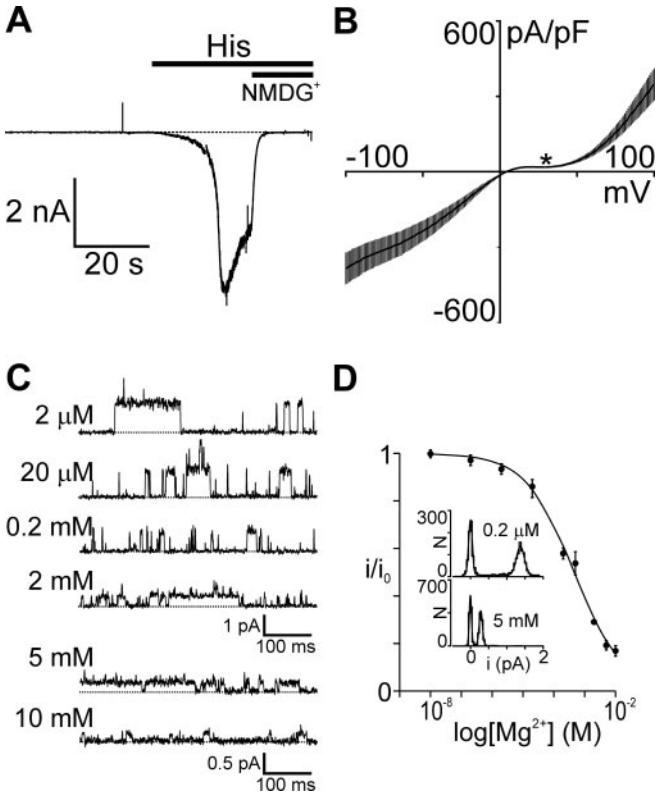

Figure 1. Mg^{2+} blocks outward currents through TRPC5 by decreasing the unitary single-channel amplitude. ***A***, Whole-cell wild-type TRPC5 currents (holding potential of −60 mV; peak amplitude density, −336.87 ± 62.74 pA/pF; time-to-peak amplitude, 18.28 ± 3.02 s; $n = 20$). Histamine (His; 10 μM) and $NMDG^+$ solution were applied as indicated. ***B***, *I–V* values taken at the peak current are averaged and displayed as the mean ± SEM ($n = 20$). ***C***, ***D***, Inhibition of TRPC5 single-channel currents by Mg^{2+} applied to the cytosolic side of inside-out membrane patches held at +30 mV (***B***, asterisk). ***C***, Sample traces of TRPC5 single-channel activity recorded in the indicated Mg^{2+} concentration (filtered at 0.5 kHz). The dotted lines indicate closed levels. At 0 and 2 mM Mg^{2+}, the mean amplitudes were 1.44 ± 0.02 pA ($n = 19$) and 0.42 ± 0.01 pA ($n = 7$), respectively. ***D***, Plot of single-channel amplitude versus $[Mg^{2+}]$. The solid line represents the fit of the data to the Hill equation ($i/i_0 = 1/(1 + ([Mg^{2+}]/IC_{50})^h)$). Each data point represents the mean amplitude of single-channel currents normalized to the mean amplitude in 0 Mg^{2+}. Inset, Two representative amplitude histograms in which the solid lines are the Gaussian fits to the histograms.

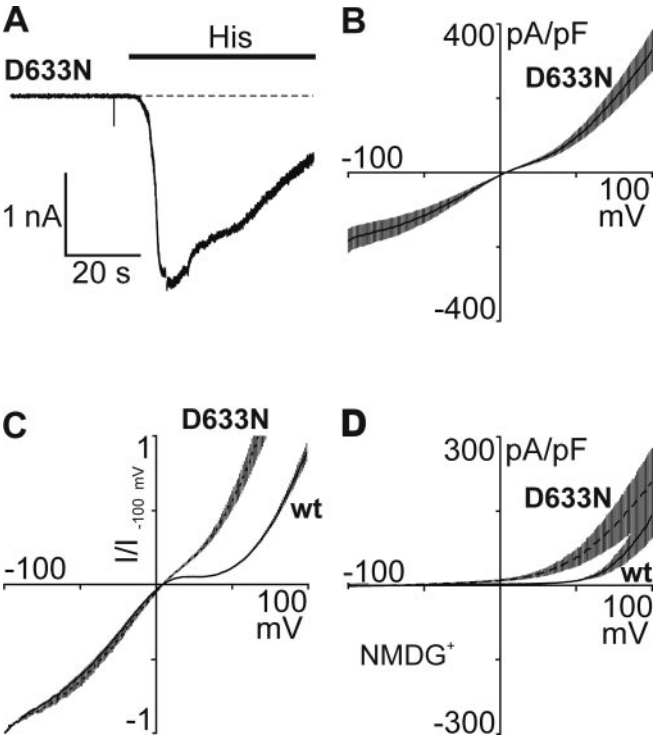

Figure 2. Aspartate 633 is responsible for the flat part of the current–voltage relationship. ***A***, Whole-cell D633N currents (holding potential, −60 mV; peak amplitude density, −149.71 ± 27.35 pA/pF; time-to-peak amplitude, 24.91 ± 4.98 s; $n = 13$). ***B***, *I–V* values are averaged and displayed as the mean ± SEM ($n = 13$). ***C***, Superimposed *I–V* values from wtTRPC5- and D633N-expressing cells normalized to the current at −100 mV. ***D***, Averaged *I–V* values of wtTRPC5 and D633N recorded in Na^+, Ca^{2+}, and Mg^{2+}-free ($NMDG^+$-containing) extracellular solution ($n = 4$ each condition). ***B***, ***C***, Taken at peak current, whereas ***D*** was taken from later in the experiment and therefore reflects rundown. His, Histamine.

−60 mV was taken for subsequent analysis. Single-channel data were filtered at 3 kHz and sampled at 10 or 100 kHz. Single-channel amplitudes were calculated from fitting Gaussian curves to the amplitude histograms. In single-channel recordings, the duration of voltage ramps from −90 to +90 mV was 94 ms. Student's *t* test was used to determine the statistical significance. Data were expressed as mean ± SEM. Although HEK293 cells express small amounts of endogenous TRPC1 and TRPC5 mRNA (Riccio et al., 2002), no currents were observed, unless cells were transfected with TRPC5 or TRPC5/TRPC1 cDNA (data not shown) (Obukhov and Nowycky, 2004), suggesting that the level of expression of the endogenous channels is very low. An excess of TRPC1 over TRPC5 cDNAs (2:1) was used to ensure predominant formation of heteromeric TRPC5/TRPC1 over homomeric TRPC5.

Experimental solutions contained the following (in mM): *whole-cell experiments*: standard extracellular solution, 150 NaCl, 1.2 $CaCl_2$, 1 $MgCl_2$, 10 HEPES, and 10 glucose, pH 7.2 (NaOH); *N*-methyl-D-glucamine ($NMDG^+$)-containing solution,150 NMDG-Cl, 10 HEPES, and 10 glucose, pH 7.2 (TrisOH); and intracellular solution, 115 Cs-MethylSO$_3$, 10 CsCl, 1 $MgCl_2$, 0.5 EGTA, and 20 HEPES, pH 7.2 (TrisOH); *single-channel experiments* (all of the solutions, pH 7.2, TrisOH): pipette solution, 140 CsCl, 2 $MgCl_2$, 1.2 $CaCl_2$, and 20 HEPES; standard bath solution, 140 CsCl, 20 HEPES, and either 2 $MgCl_2$ or 2 *N*-(2-hydroxyethyl)ethylenediaminetriacetic acid (HEDTA); Mg^{2+} block bath solution, 140 CsCl, 20 HEPES, and 7 HEDTA (0–0.00001 Mg^{2+}), 7 HEDTA and 0.025 $MgCl_2$ (0.0002 Mg^{2+}), 7 HEDTA and 0.248 $MgCl_2$ (0.002 Mg^{2+}), 5 HEDTA and 1.356 $MgCl_2$ (0.02 Mg^{2+}), 4 HEDTA and 3.34 $MgCl_2$ (0.2 Mg^{2+}), 0.5 $MgCl_2$ (0.5 Mg^{2+}), 2 $MgCl_2$ (2 Mg^{2+}), 5 $MgCl_2$ (5 Mg^{2+}), and 10 $MgCl_2$ (10 Mg^{2+}). Numbers in parentheses indicate values of free Mg^{2+} as a millimolar concentration (Schubert, 1996).

Results

Mg^{2+} block of outward currents in TRPC5 channels

Histamine evoked large inward currents in HEK293 cells transfected with wild-type TRPC5 (wtTRPC5) and H_1R (Fig. 1*A*). The current developed over 10–20 s to a peak amplitude, which then decayed slowly and variably, as described previously (Obukhov and Nowycky, 2004). Inward currents were abolished after the substitution of all of the extracellular small cations with $NMDG^+$ (Fig. 1*A*), confirming that TRPC5 current is cationic. *I–V* relationships, obtained by applying voltage ramps from −100 to +100 mV, were doubly rectifying (Fig. 1*B*) and displayed the characteristic "flat" segment with a near-zero slope between +10 and +40 mV that has been attributed to $[Mg^{2+}]_i$ block in TRPC5 and TRPC4 channels (Schaefer et al., 2000).

To verify Mg^{2+} block, we performed single-channel experiments using inside-out membrane patches from cells expressing wtTRPC5. TRPC5 channel activity was stimulated by adding 1–10 μM GTPγS and 2 mM $[Mg^{2+}]_i$ to the cytosolic side of excised patches. Subsequently, membrane patches were exposed to solutions containing various concentrations of free Mg^{2+} (see

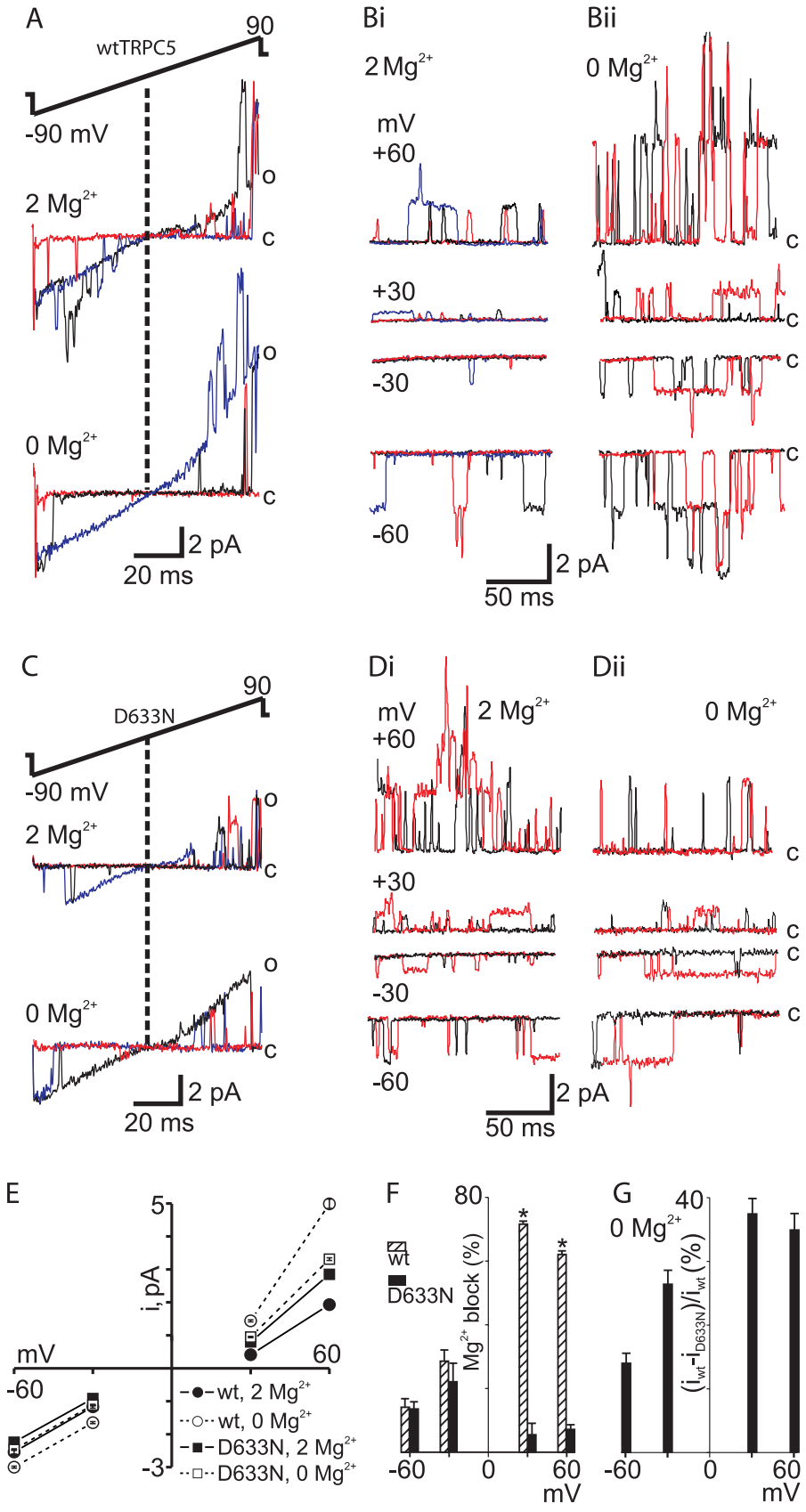

Materials and Methods). Experiments were performed with patches held at +30 mV (Fig. 1*B*, asterisk).

Mg^{2+} markedly decreased the amplitude of unitary single-channel currents (Fig. 1*C*,*D*), suggesting that Mg^{2+} is a "fast blocker" (Hille, 2001). A fit of the dose–response curve with the Hill equation yielded an IC_{50} of 457 μM for $[Mg^{2+}]_i$, with a Hill coefficient of 0.6 (Fig. 1*D*), suggesting a slight negative cooperativity. $[Mg^{2+}]_i$ had little or no effect on channel open probability (NP_o). Indeed, NP_o was slightly greater at higher $[Mg^{2+}]_i$ (2 or 5 mM), although this did not reach statistical significance [NP_o at 5 mM, 0.34 ± 0.19 ($n = 3$) vs NP_o at 200 nM, 0.08 ± 0.04 ($n = 5$); $p > 0.05$]. Thus, we conclude that $[Mg^{2+}]_i$ block of outward currents through TRCP5 homomers results from a decrease of single-channel unitary amplitudes.

Mutation of aspartate 633 abolishes the zero-slope segment of the *I–V* relationship

Because TRPC5 lacks anionic residues in the putative pore region, it is unlikely that Mg^{2+} block is mediated within the transmembrane region. Therefore, we examined three negatively charged residues (D633, D636, and E638) situated near the predicted termination of TM6 (Dohke et al., 2004) by making single point mutations. The E638 residue belongs to a short, highly conserved motif called the "TRP box" (EWKFAR) (Clapham, 2003). The substitution of this residue with glutamine resulted in nonfunctional channels (data not shown), and the mutant was not studied further.

Mutation of the D633 residue to asparagine (D633N) resulted in a channel with robust activity. Histamine-evoked currents through the D633N TRPC5 mutant exhibited slow activation and variable decay kinetics similar to those of wtTRPC5 (Fig. 2*A*). The *I–V* relationship of the D633N channel, however, was strikingly different (Fig. 2*B*). At +10 to +40 mV, at which the *I–V* values from wtTRPC5 were relatively flat, the *I–V* of D633N increased approximately linearly. Above +40 mV, the outward currents of both channels increased supralinearly. Normalization of the traces from wtTRPC5 and D633N to currents at −100 mV demonstrates the *I–V* differences more clearly (Fig. 2*C*). The substitution of external cations with $NMDG^+$ eliminated all of the inward currents through both wtTRPC5 or D633N, revealing a prominent outward curvature at positive potentials (Fig. 2*D*). The out-

Figure 3. Aspartate 633 is critical for Mg^{2+} block of single-channel currents. Single-channel recordings from inside-out patches of wtTRPC5- (***A***, ***B***) and D633N- (***C***, ***D***) transfected HEK293 cells. ***A***, Ramps from −90 to +90 mV demonstrate *I–V* relationships through open channels. The bath solution contained 2 mM $MgCl_2$ or 2 mM HEDTA (0 Mg^{2+}). c, Closed; o, open. In each panel, three traces are superimposed and shown in different colors for clarity. ***B***, Voltage steps were applied to potentials indicated at left. NP_o levels were 1.15 ± 0.23 versus 0.65 ± 0.17 [2 mM ($n = 6$) vs 0 Mg^{2+} ($n = 17$) at +60 mV; (*Figure legend continues.*)

ward currents of D633N channels were detected as negative as −50 mV, whereas currents through wtTRPC5 channels were strongly suppressed until approximately +40 mV (Fig. 2*D*). These experiments indicate that residue D633 is an important determinant of the unique conductivity properties of TRPC5.

D633 mediates Mg^{2+}-dependent block of TRPC5 outward currents

To confirm that D633 mediates $[Mg^{2+}]_i$ block of TRPC5, we turned to single-channel recordings. Membrane patches were excised from cells expressing either wtTRPC5 or the D633N variant, and experiments were performed as in Figure 1*C*.

At 2 mM Mg^{2+}, wtTRPC5 single-channel current amplitudes during voltage ramps resembled the *I–V* relationship obtained in whole-cell recordings. The current amplitude (*i*) varied linearly with voltage at negative potentials, was barely resolved between +10 and +40 mV, and increased at more positive potentials (Fig. 3*A*, 2 Mg^{2+}). In Mg^{2+}-free bath solution, single-channel *I–V* values were linear at negative potentials; however, at positive potentials, single-channel events were larger and amplitudes increased throughout the whole range from 0 to +90 mV (Fig. 3*A*, 0 Mg^{2+}). To perform a quantitative analysis, we stepped the voltage to four potentials (Fig. 3*B*). At negative potentials (−60 and −30 mV), single-channel current amplitudes recorded in Mg^{2+}-containing and Mg^{2+}-free solutions were similar (Fig. 3*B*); however, at positive potentials, they were markedly larger in Mg^{2+}-free solutions (Fig. 3*B*,*E*). In contrast to wtTRPC5, D633N single-channel current amplitudes exhibited little Mg^{2+} dependence (Fig. 3*C*,*D*). During both voltage ramps and voltage steps, the current amplitudes were similar in Mg^{2+}-containing and Mg^{2+}-free solutions (Fig. 3*C*,*D*). There was no significant difference between NP_o of either wt or D633N channels, in either the presence or absence of Mg^{2+} ions.

The single-channel amplitudes for both channels were compared in an *i–V* plot (Fig. 3*E*). The potency of Mg^{2+} block on the channels is summarized in Figure 3*F*. In wtTRPC5 channels, removal of Mg^{2+} profoundly increases the single-channel amplitude at positive potentials. In contrast, in the D633N mutant, Mg^{2+} ions have a small effect on single-channel amplitude at all of the potentials (≤25%). Thus, the substitution of a polar asparagine for the negatively charged D633 effectively eliminates voltage-dependent Mg^{2+} block of TRPC5 at positive potentials.

The *i–V* plot also illustrates that, although D633N unitary amplitudes are considerably larger than those of wtTRPC5 at positive potentials in 2 mM Mg^{2+} solution, they are smaller than unitary amplitudes of wtTRPC5 in Mg^{2+}-free solution at all of the potentials (Fig. 3*E*), suggesting that the mutation has additional effects on conductance. To analyze this phenomenon, we compared single-channel current amplitudes of wt and mutant TRPC5 in Mg^{2+}-free solution (Fig. 3*G*). The amplitudes of D633N single-channel currents are ~30–35% smaller than those of wtTRPC5 at three potentials, with somewhat less difference at −60 mV. This result suggests that, in addition to mediating voltage-dependent Mg^{2+} block, the residue may have effects on conductivity properties. To test this, we constructed additional mutants.

Cytosolic residues 633 and 636 regulate TRPC5 current amplitude

First, we substituted alanine, a nonpolar neutral residue, for aspartate at position 633. The *I–V* of D633A did not exhibit the flat part at positive potentials between +10 and +40 mV (Fig. 4*A*), consistent with elimination of Mg^{2+} block. Inward currents were very small in D633A compared with outward currents.

Subsequently, we tested the consequences of replacing D633 with a positively charged residue, lysine (Fig. 4*B*). The D633K mutation completely eliminated currents at negative potentials, indicating that the positive charge blocked the inward movement of cations through the conduction pathway. Nevertheless, small outward currents were observed at potentials more positive than approximately +40 to +50 mV. This current was unchanged by the substitution of extracellular Cl^- ($n = 3$; data not shown), indicating that it represented the outward flow of cations.

We also investigated the effect of a residue bearing a negative charge, but with a different side chain length, by substituting D633 with glutamate. At positive potentials, the D633E *I–V* resembled the *I–V* of wtTRPC5 (Fig. 4*C*), with a flat part between +10 and +40 mV. At negative potentials, the *I–V* values of D633E currents were small relative to the outward current at +100 mV. These results suggest that a longer side chain bearing a negative charge interferes with inward currents but mediates Mg^{2+} block and permits outward current at positive potentials.

To examine whether the Mg^{2+} sensitivity of TRPC5 is confined to the D633 residue, we constructed a D636N mutant. D636N exhibited a wtTRPC5-like *I–V* with a well defined flat part between +10 and +40 mV (Fig. 4*D*). However, as for D633E, the inward currents in the D636N *I–V* were small relative to the outward current at +100 mV. We conclude that D636 does not mediate the voltage-dependent Mg^{2+} block of TRPC5 but exerts an effect on cation entry at negative potentials.

TRPC5/TRPC1 heteromer conductivity differs from TRPC5 homomers

In native cells, TRPC5 can form heteromers with TRPC1 (Strübing et al., 2001; Greka et al., 2003). In contrast to homomeric TRPC5, the TRPC5/TRPC1 heteromer has unique conductivity properties, including a very small inward current and nearly linear *I–V* at positive potentials (Strübing et al., 2001). Sequence alignment revealed that a TRPC1 asparagine, N670, occupies the equivalent location to D633 in TRPC5, whereas the D636 and E638 equivalent positions are conserved (Fig. 4*E*). We asked whether the difference in *I–V* relationship was attributable to the lack of aspartate at position 670 of TRPC1. Cells were cotransfected with wild-type TRPC1 and TRPC5. We verified the formation of heteromers by determining the *I–V* characteristics in our recording conditions (Fig. 4*F*). Histamine evoked currents whose *I–V* relationship was essentially identical to those described for muscarinic activation of a TRPC5/TRPC1 current (Strübing et al., 2001; Bezzerides et al., 2004). Subsequently, we coexpressed the TRPC1 N670D mutant with wtTRPC5. The *I–V* relationship of wtTRPC5/N670D was not significantly different from the

←

(*Figure legend continued.*) $p > 0.05$]. ***C***, ***D***, Parallelexperiments to ***A*** and ***B***, respectively, for patches excised from D633N-transfected cells. NP_o levels were 0.82 ± 0.12 versus 0.99 ± 0.13 [2 mM ($n = 17$) vs 0 Mg^{2+} ($n = 20$) at +60 mV; $p > 0.05$]. ***B***, ***D***, Data were filtered at 0.5 kHz. ***E***, Plot of averaged single-channel amplitudes obtained from voltage-step experiments (n = 6–20; SEMs are smaller than symbols). At +30 mV, the D633N mean amplitudes were 0.80 ± 0.03 pA ($n = 17$; 2 mM Mg^{2+}) and 0.95 ± 0.02 pA ($n = 20$; 0 Mg^{2+}). ***F***, Comparison of Mg^{2+} block of wtTRPC5 ($n = 6$) versus D633N ($n = 9$). ***G***, Comparison of single-channel amplitudes of wtTRPC5 ($n = 6$) versus D633N ($n = 6$) in 0 Mg^{2+}. ***F***, wt and D633N single-channel amplitudes were significantly different at +30 and +60 mV (*$p < 0.01$) but were similar at −30 and −60 mV ($p > 0.05$). Error bars indicate SEM. ***G***, The single-channel amplitude of D633N mutants was significantly different from wtTRPC5 at all four of the potentials ($p < 0.01$).

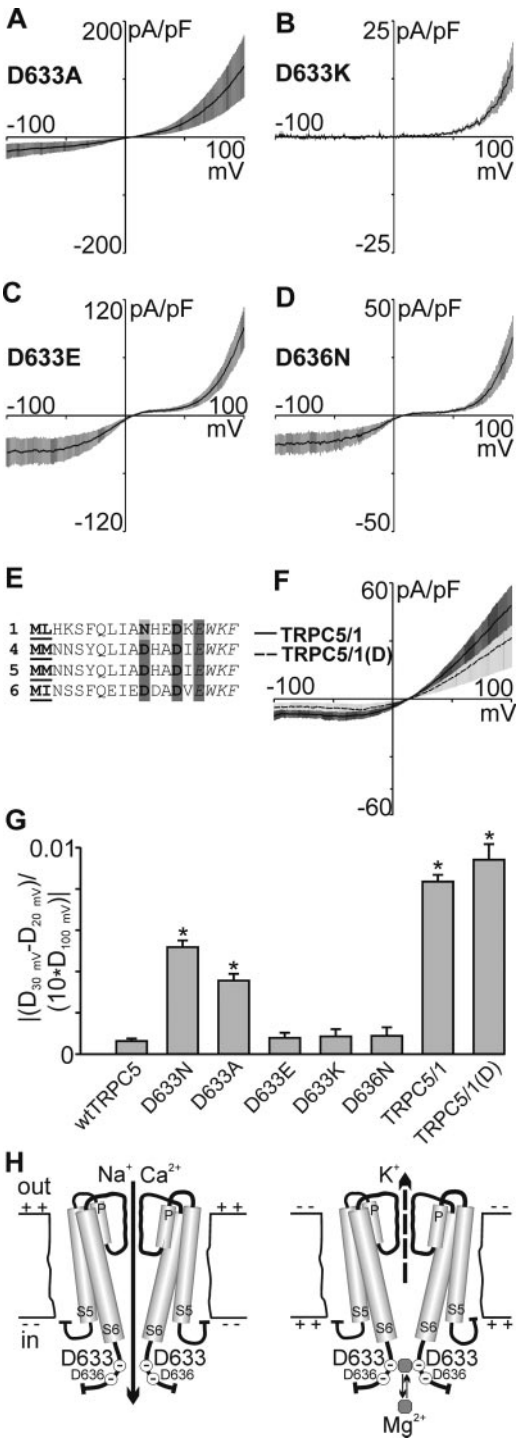

Figure 4. Effect of the substitutions of D633, D636, and TRPC5/TRPC1 heteromer formation on Mg^{2+} block and inward currents. Averaged whole-cell *I–V* values of D633A ($n = 6$; ***A***), D633K ($n = 7$; ***B***), D633E ($n = 8$; ***C***), D636N ($n = 6$; ***D***), and TRPC5/TRPC1 ($n = 8$; ***F***) and TRPC5/TRPC1(D) heteromers ($n = 4$; ***F***) are shown as solid or dashed lines. ***E***, An alignment of the sequence of TRPC1, TRPC4, TRPC5, and TRPC6 for a segment between the end of TM6 (underlined) and the TRP box (italicized). Identical aspartates and glutamates are marked in gray. ***G***, Slopes of *I–V* values between +20 and +30 mV are normalized to the current density at +100 mV and serve as a measure of the sensitivity of mutants and heteromers to Mg^{2+}. TRPC5/1(D) indicates heteromers of TRPC5 and TRPC1(N670D) mutant. $*p < 0.05$. Error bars indicate SEM. ***H***, A model of the TRPC5 cation conduction pathway at negative (left) and positive (right) potentials. For clarity, only two subunits are shown. D633 and D636 are designated as open circles, whereas Mg^{2+} is shown as an octagon. The bold arrows indicate the direction of cation fluxes. The thin arrows indicate that Mg^{2+} is a fast blocker. P, P-helix; S5, TM5; S6, TM6; ++, positively charged; −−, negatively charged.

I–V of the wild-type heteromer (Fig. 4*F*, dashed line). This indicates that TRPC5/TRPC1 heteromers have additional structural differences that account for the conductivity properties of the channel and distinguish them from TRPC5 homomers.

To compare quantitatively the effectiveness of Mg^{2+} block in the homomeric and heteromeric channels described above, we calculated the slopes of the *I–V* values between +20 and +30 mV and normalized them to the current amplitude density at +100 mV to offset differences in the expression level of the mutants. The normalized slopes in D633N, D633A, wtTRPC5/wtTRPC1, and wtTRPC5/N670D were significantly larger than in wtTRPC5, D633K, D633E, and D636N (Fig. 4*G*) ($p < 0.05$). These data support our hypothesis that the interaction between Mg^{2+} and a negatively charged residue plays a crucial role in mediating the Mg^{2+} block of TRPC5.

Discussion

Here, we demonstrate that residue D633 is a critical determinant of TRPC5 conductivity properties. Numerous lines of evidence suggest that TRPC channels are assembled from four subunits, each with six transmembrane domains (Clapham, 2003). Recent experiments on TRPC1 strongly support a model in which the sixth TM domain of TRPC channels is terminated at a location corresponding to M624 in TRPC5 (Dohke et al., 2004). Based on the data and structural models for other cation channels (Bichet et al., 2003), we propose that D633 residues of homomeric TRPC5 are a cytoplasmic continuation of the conduction pathway, forming an inner vestibule of the channel (Fig. 4*H*).

Negatively charged residues can form rings surrounding the main channel axis and mediate critical functional properties (Doyle, 2004). Negatively charged rings can be found in extracellular, transmembrane, or intracellular domains of many cation channels (Imoto et al., 1988; Kuo et al., 2003; Miyazawa et al., 2003). Strategically located anionic rings enhance channel conductivity by electrostatic attraction of positively charged ions. In some channels, the rings additionally mediate block by extracellular or intracellular Mg^{2+}. In the TRP family, TRPV5 and TRPV6 are strongly inwardly rectifying and Mg^{2+} blocks the channel at a charged residue within the transmembrane pore region (Nilius et al., 2001; Voets et al., 2003). Several Kir channels have Mg^{2+}-sensitive, negatively charged rings in both the pore and cytoplasmic domains (Yang et al., 1995; Kubo and Murata, 2001; Kuo et al., 2003). The TRPC5 homomer shares some of the features of an inward rectifier: block by intracellular Mg^{2+} at physiological potentials and a relatively large inward current. Mg^{2+} block appears to be mostly mediated by D633 but not D636 residues, whereas the conductivity of the channel seems to depend on both of these anionic residues (Fig. 4*D*,*H*). D633 residues may form an anionic ring; however, other models are not excluded by our data.

Mg^{2+} block of homomeric TRPC5 is relieved at strongly positive potentials. At least two models have been proposed to explain the relief of block mediated by fast-blocking cations. According to the punch-through model (Woodhull, 1973), the blocking cation permeates through the pore at high voltages. A second model invokes a repulsion mechanism (Heginbotham and Kutluay, 2004) and suggests that destabilization of blocker binding to its site may result from repulsion between the charged blocker and permeant cations occupying adjacent sites within the inner selectivity filter of the pore. Both mechanisms might play a role in mediating the relief of Mg^{2+} block in TRPC5.

We propose a third possible mechanism, that the segment of TRPC5 bearing the D633 residue is not rigid but can be moved or

twisted away from the main channel axis. We base this hypothesis on the observation of significant outward currents through all of the mutant channels tested, including D633K with positively charged lysine and D633A with neutral alanine substitution, at potentials similar to those that relieve Mg^{2+} block in wtTRPC5. Mutation D633K abolishes all of the inward currents. If residue K633 were immobile relative to the conduction pathway, the D633K mutant should carry neither outward nor inward currents at all of the voltages. In the proposed model, strongly positive potentials would distort the arrangement of residues at location 633 sufficiently to allow outward conduction of cations. However, additional experiments are necessary to distinguish between the various hypotheses.

In summary, we conclude that a single cytosolic residue, D633, situated nine residues beyond the end of the TM6 domain, has a powerful role in shaping the conduction properties of TRPC5 by both mediating $[Mg^{2+}]_i$ block and modulating the magnitude of the relative inward cation current. TRPC4 and TRPC6 also exhibit similar voltage-dependent sensitivity to $[Mg^{2+}]_i$ (Clapham, 2003). Both channels possess aspartates at positions equivalent to D633 (Fig. 3*D*), and anionic rings at this location may shape the properties of TRPC4 and TRPC6 as well. The conductivity properties of the TRPC5/TRPC1 heteromer contrast strikingly with those of the TRPC5 homomer, including lack of Mg^{2+} sensitivity and small inward currents. We propose that at least some of the heteromeric properties may be attributable to structural distortion of the putative D633 ring formed by TRPC5 monomeric assembly. The configuration of anionic rings in TRPC channels may be exploited for the formation of heteromers with strikingly different physiological properties and may be subject to modulation by second-messenger systems.

References

Bezzerides VJ, Ramsey IS, Kotecha S, Greka A, Clapham DE (2004) Rapid vesicular translocation and insertion of TRP channels. Nat Cell Biol 6:709–720.

Bichet D, Haass FA, Jan LY (2003) Merging functional studies with structures of inward-rectifier K^+ channels. Nat Rev Neurosci 4:957–967.

Clapham DE (2003) TRP channels as cellular sensors. Nature 426:517–524.

Dohke Y, Oh YS, Ambudkar IS, Turner RJ (2004) Biogenesis and topology of the transient receptor potential Ca^{2+} channel TRPC1. J Biol Chem 279:12242–12248.

Doyle DA (2004) Structural themes in ion channels. Eur Biophys J 33:175–179.

Greka A, Navarro B, Oancea E, Duggan A, Clapham DE (2003) TRPC5 is a regulator of hippocampal neurite length and growth cone morphology. Nat Neurosci 6:837–845.

Heginbotham L, Kutluay E (2004) Revisiting voltage-dependent relief of block in ion channels: a mechanism independent of punchthrough. Biophys J 86:3663–3670.

Hille B (2001) Ion channels of excitable membranes, Chap 16, Ed 3. Sunderland, MA: Sinauer.

Imoto K, Busch C, Sakmann B, Mishina M, Konno T, Nakai J, Bujo H, Mori Y, Fukuda K, Numa S (1988) Rings of negatively charged amino acids determine the acetylcholine receptor channel conductance. Nature 335:645–648.

Kubo Y, Murata Y (2001) Control of rectification and permeation by two distinct sites after the second transmembrane region in Kir2.1 K^+ channel. J Physiol (Lond) 531:645–660.

Kuo A, Gulbis JM, Antcliff JF, Rahman T, Lowe ED, Zimmer J, Cuthbertson J, Ashcroft FM, Ezaki T, Doyle DA (2003) Crystal structure of the potassium channel KirBac1.1 in the closed state. Science 300:1922–1926.

Miyazawa A, Fujiyoshi Y, Unwin N (2003) Structure and gating mechanism of the acetylcholine receptor pore. Nature 423:949–955.

Moran MM, Xu H, Clapham DE (2004) TRP ion channels in the nervous system. Curr Opin Neurobiol 14:362–369.

Nilius B, Vennekens R, Prenen J, Hoenderop JG, Droogmans G, Bindels RJ (2001) The single pore residue Asp542 determines Ca^{2+} permeation and Mg^{2+} block of the epithelial Ca^{2+} channel. J Biol Chem 276:1020–1025.

Obukhov AG, Nowycky MC (2002) TRPC4 can be activated by G-protein-coupled receptors and provides sufficient Ca^{2+} to trigger exocytosis in neuroendocrine cells. J Biol Chem 277:16172–16178.

Obukhov AG, Nowycky MC (2004) TRPC5 activation kinetics are modulated by the scaffolding protein ezrin/radixin/moesin-binding phosphoprotein-50 (EBP50). J Cell Physiol 201:227–235.

Riccio A, Medhurst AD, Mattei C, Kelsell RE, Calver AR, Randall AD, Benham CD, Pangalos MN (2002) mRNA distribution analysis of human TRPC family in CNS and peripheral tissues. Mol Brain Res 109:95–104.

Schaefer M, Plant TD, Obukhov AG, Hofmann T, Gudermann T, Schultz G (2000) Receptor-mediated regulation of the nonselective cation channels TRPC4 and TRPC5. J Biol Chem 275:17517–17526.

Schubert R (1996) Multiple ligand-ion solutions: a guide for solution preparation and computer program understanding. J Vasc Res 33:86–98.

Strübing C, Krapivinsky G, Krapivinsky L, Clapham DE (2001) TRPC1 and TRPC5 form a novel cation channel in mammalian brain. Neuron 29:645–655.

Voets T, Janssens A, Prenen J, Droogmans G, Nilius B (2003) Mg^{2+}-dependent gating and strong inward rectification of the cation channel TRPV6. J Gen Physiol 121:245–260.

Woodhull A (1973) Ionic blockage of sodium channels in nerve. J Gen Physiol 61:687–708.

Yang J, Jan YN, Jan LY (1995) Control of rectification and permeation by residues in two distinct domains in an inward rectifier K^+ channel. Neuron 14:1047–1054.